2020 IEEE/RSJ International Conference on Intelligent Robots and Systems (IROS)
October 25-29, 2020, Las Vegas, NV, USA (Virtual)

Supervised Semi-Autonomous Control for Surgical Robot Based on Bayesian Optimization

Junhong Chen*, Dandan Zhang*, *Student Member, IEEE*, Adnan Munawar, Ruiqi Zhu, Benny Lo, *Senior Member, IEEE*, Gregory S. Fischer, Guang-Zhong Yang, *Fellow, IEEE*

***Abstract*— The recent development of Robot-Assisted Minimally Invasive Surgery (RAMIS) has brought much benefit to ease the performance of complex Minimally Invasive Surgery (MIS) tasks and lead to more clinical outcomes. Compared to direct master-slave manipulation, semi-autonomous control for the surgical robot can enhance the efficiency of the operation, particularly for repetitive tasks. However, operating in a highly dynamic *in-vivo* environment is complex. Supervisory control functions should be included to ensure flexibility and safety during the autonomous control phase. This paper presents a haptic rendering interface to enable supervised semi-autonomous control for a surgical robot. Bayesian optimization is used to tune user-specific parameters during the surgical training process. User studies were conducted on a customized simulator for validation. Detailed comparisons are made between with and without the supervised semi-autonomous control mode in terms of the number of clutching events, task completion time, master robot end-effector trajectory and average control speed of the slave robot. The effectiveness of the Bayesian optimization is also evaluated, demonstrating that the optimized parameters can significantly improve users' performance. Results indicate that the proposed control method can reduce the operator's workload and enhance operation efficiency.**

I. Introduction

The advent of Robotic-Assisted Minimally Invasive Surgery (RAMIS) has brought much benefit to help realize the full potential of MIS. Most of the existing robotic platforms for RAMIS are developed based on master-slave control [1], [2]. For example, the da Vinci Surgical System (dVSS) can be regarded as a representative. Surgeons can benefit from its endo wrist design for dexterous operation. The functions of tremors removal and motion scaling can enable precise operation during robotic surgery. However, no autonomy is incorporated in the dVSS. The current trend for surgical robots development is towards safer, smaller, smarter embodiment to ensure wider clinical uptake [3] in the years to come. In pursuit of a higher level of autonomy, Artificial Intelligent (AI) can be incorporated into current surgical operation workflow [4].

The semi-autonomous robot can reduce the cognitive load of the operator and potentially shorten the operation time, which enables the surgeons to focus on the most critical tasks and lessen the fatigue for repetitive tasks [5]. Given the advances in surgical robotic technologies, collaborative working between surgeons and robotic systems will lead to better clinical outcomes. For example, a robot can operate precisely and stably given the desired task, while human guidance can ensure safety, make diagnostic and procedural decisions, and adjust the operation according to the patient's anatomy and situations. Moreover, a human operator can conduct complex operations through fine-tuning control and handle the emergency with decision-making. Therefore, to enable the human operator to maintain the control of the robot, a shared control method can be designed to enable semi-autonomous control.

The importance of adjustable roles during human-robot interaction has been emphasized in [6]. Though the concept of human-robot cooperative control has already been implemented in a master-slave paradigm [7], the role adaption between the human and the robot during semi-autonomous control has not been fully exploited.

Some of the existing autonomous surgical systems provide supervisory functions in different modes. These include the preoperative model acquisition or computer-assisted surgical planning, such as planning, teaching, monitoring, and intervening [8], [9]. Suppose that the control input is generated by the operator and the robot, the level of control assigned to the operator and the robot can be adjusted to facilitate a smooth workflow in a surgical operation. The human control input during the autonomous mode can be defined as supervisory functions for semi-autonomous control.

For human-in-the-loop control, user-specific parameters require fine-tuning. Bayesian optimization is a common method for nonlinear optimization [10] for applications which involve human-robot interaction [11]. It is a data-efficient approach [12], since only a few samples are needed for optimization [13]. Therefore, in this work, Bayesian optimization is used to tune the parameters for the user-specific role adaption between the human operator and the robot during an autonomous task.

The proposed supervised semi-autonomous control method based on Bayesian optimization is validated with a customized simulator based on a peg transfer task, while comparisons were made to assess the differences between with and without using the supervised semi-autonomous control method. Further user studies are conducted to evaluate the effectiveness of the Bayesian optimization.

The remainder of this paper is organized as follows. Section II introduces the implementation of the semi-autonomous control method. The adaptive mechanism is

*These authors contributed to this paper equally.

J. Chen, D. Zhang, R. Zhu, B. Lo and G.-Z. Yang are with the Hamlyn Centre for Robotic Surgery, Imperial College London, London, United Kingdom. G.-Z. Yang is also with the Institute of Medical Robotics, Shanghai Jiao Tong University, China. A. Munawar and G.S. Fischer are with the Worcester Polytechnic Institute, Worcester, Massachusetts, USA. email:d.zhang17@imperial.ac.uk.

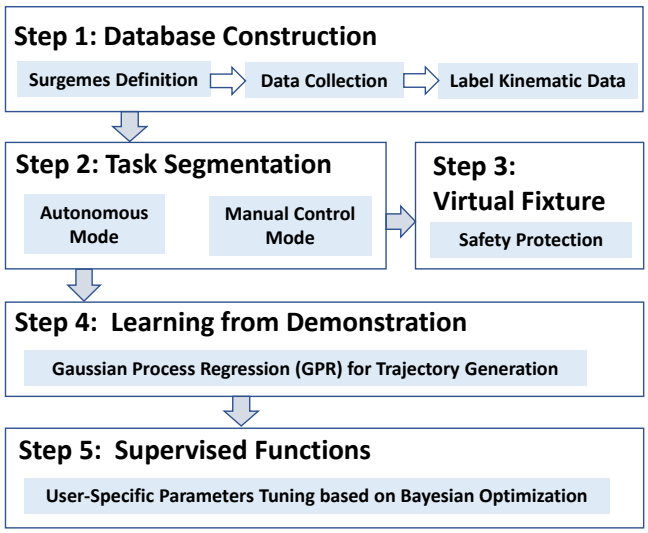

Fig. 1. The general steps of the proposed supervised semi-autonomous control.

described in detail, as it leads to the construction of the supervised semi-autonomous control. Moreover, the user-specific parameters tuning based on Bayesian optimization is introduced. Section III presents the user study design and results analysis. Conclusions are drawn in Section IV.

II. Methodology

In this section, the key procedures of the implementation of the proposed semi-autonomous control are illustrated. The supervisory function is introduced to facilitate the supervised semi-autonomous control. The user-specific parameters tuning based on Bayesian Optimization is introduced.

A. Overview

The overall workflow of the supervised semi-autonomous control is illustrated in Fig. 1. The first step is database construction with data registration and labelling. The second step is task segmentation, which divides a surgical procedure into two phases that require different control modes, i.e. i) manual control by the operator, ii) autonomous execution of a pre-defined trajectory. The manual control can be realized based on the traditional master-slave with suitable motion scaling to ensure precision for fine control. Virtual fixture is incorporated into the control for safety consideration, which can be regarded as the third step. With virtual fixture, the risk of tissue damage can be reduced. The autonomous control phase is built with learning from demonstration (LfD), which is the fourth step. LfD can generate the desired trajectory for task automation, which is an effective method in pursuit of a higher level of autonomy [14]. The final step is incorporating the supervisory functions to achieve supervised semi-autonomous control. More details about task segmentation, model regression for desired trajectory generation, the implementation of semi-autonomous control and the supervisory functions are described in the following subsections.

Due to the difference in the user's experience and control preferences, the proposed semi-autonomous control method has to be tuned to suit each individual user. Therefore, Bayesian optimization is required to improve this control scheme in a user-specific manner.

B. Task Segmentation

Surgical tasks can be decomposed into basic rudimentary gestures, named surgemes [15]. For example, seven types of surgemes are defined for the ring transfer task in [16], while fifteen types of surgemes for the knot-tying task, the suturing task and the needle-passing task have been defined in JIGSAW(JHU-ISI Gesture and Skill Assessment Working Set) [17]. Based on the characteristics of different tasks, the surgemes can be further divided into coarse motions and fine movements [16], [18]. The surgemes used in this paper is defined in Table I.

TABLE I
The definitions of surgemes for the peg transfer task.

Index	Description	Type
P1	Lifting object with right-hand tool	Precise motion
P2	Lifting object with left-hand tool	Precise motion
P3	Moving with right-hand tool	Coarse motion
P4	Moving with left-hand tool	Coarse motion
P5	Placing object with right-hand tool	Precise motion
P6	Placing object with left-hand tool	Precise motion
P7	Transferring object from right to left	Precise motion
P8	Transferring object from left to right	Precise motion

Fine movements include bimanual operation, which requires the control of two surgical tools during the operation. As for coarse motions, the gross positioning, moving the surgical tool to another distant target for operation, transferring the object from one position to another. These procedures can be performed by the robot automatically with enhanced efficiency and reduced errors to the desired path. For example, P3 and P4 refer to coarse motions while the others represent fine motions respectively in this paper.

After constructing the database, the kinematic data can be manually annotated with specific surgemes defined at the frame level by analyzing the video. The kinematic data of the coarse surgemes can then be selected from the database to train a model for trajectory regression based on LfD, which paves a way for the implementation of the autonomous execution phase.

C. Model Regression

Gaussian Process Regression (GPR) is a nonparametric Bayesian approach for regression, which is a data-efficient method and can allow uncertainty during predictions. With the limited training data, GPR can calculate the posterior and compute the predictive posterior distribution on the desired points.

Suppose that t represents the time step, $\boldsymbol{P}$ is the trajectory comprised of n time steps obtained during the demonstration phase, where $p = [x, y, z]$ ($p = \boldsymbol{P}(t)$). $p^* = [x^*, y^*, z^*]$ is the desired location for the regressed model, which can be

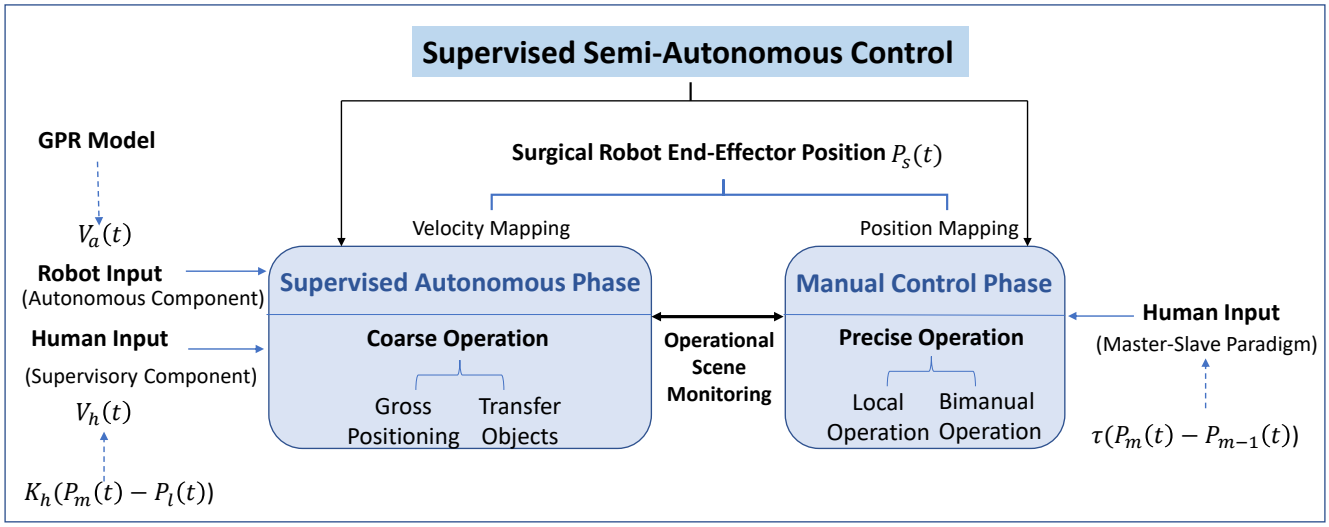

Fig. 2. The overview of the supervised semi-autonomous control framework.

known as the test observation. $f(p^*)$ is the prediction result based on Gaussian Process.

A Gaussian process prior, specified using a mean function and a covariance function is described by (1). With an infinite-dimensional multivariate Gaussian distribution, all the data in the training set are joint Gaussian distributed.

$$f(p) \sim GP(M(p), K(p, p^*)) \tag{1}$$

where $M(p) = \mathbb{E}(f(p))$, $K(p, p^*) = \mathbb{E}(f(p) - M(p))(f(p^*) - M(p^*))(p = x, y, z$ respectively). A kernel is required to generate the covariance matrix K. In this paper, we used the squared exponential kernel.

Considering that the training data may be noisy, we assume that $f(p)$ contains additive independent identically distributed Gaussian noise ϵ with variance σ_n^2. After normalization to ensure prior mean distribution of zero, the prior of the distribution of joint $f(p)$ and $f(p^*)$ can be obtained. The predictive distribution can be generated based on conditioning the joint Gaussian prior distribution on the observations [19].

The Gaussian process can model a sequence of observations, such as the desired trajectory of the surgical robot end-effector. Therefore, we implement GPR to realize autonomous phase in this paper.

D. Semi-Autonomous Control

Semi-autonomous control includes two phases, i.e. i) manual control phase, ii) autonomous phase. The overview of the supervised semi-autonomous control framework is shown in Fig. 2.

1) Manual Control Phase: For the manual control phase, in order to achieve intuitive control of the slave robot, the orientation of the end-effector of the slave robot is the same as that of the master controller. As for the position control during the manual control phase, the master end-effector displacement and the position of the end-effector of the slave robot are the control input and output respectively. The position change of the master is mapped to the slave by a scaling factor τ for more precise control of the end-effector with fine movements. The end-effector position $\boldsymbol{p_s(t)}$ at time step t can be calculated as follows.

$$\boldsymbol{p_s(t)} = \boldsymbol{p_s(0)} + \tau(\boldsymbol{p_m(t)} - \boldsymbol{p_m(0)}) \tag{2}$$

where $\boldsymbol{p_m(t)}$ is the end-effector position of the master controller at time step t.

During fine operation, virtual fixture is used to ensure safe operation where movement constraints are introduced with force feedback, since bimanual operation should avoid the collision between the two surgical tools. As for the tool-tissue interaction, delicate manipulation is required. With virtual fixture, the potential damages to critical anatomical structures can be avoided by limiting the force exerting on the tissue during a surgical operation.

2) Autonomous Phase: As for the autonomous phase, the robot takes the lead and executes the learned trajectory, which is generated based on GPR. $\boldsymbol{v_a(t)}$ is the autonomous control component generated by the robot based on the predefined trajectory. Suppose that $\boldsymbol{P_a(t)}$ is the desired trajectory generated by the GPR model, $\boldsymbol{v_a(t)} = (\boldsymbol{P_a(t)} - \boldsymbol{P_a(t-1)})/\Delta t$, where Δt is the time increment. Therefore, the end-effector position $\boldsymbol{p_s(t)}$ at time step t can be calculated as follows.

$$\boldsymbol{p_s(t)} = \boldsymbol{p_s(t-1)} + \boldsymbol{v_a(t)}\boldsymbol{\Delta t} \tag{3}$$

The velocity profile of the autonomous surgical tool control is important to be explored. The initial velocity is set to zero at the control phase switching point. When the control mode is switched from manual mode to autonomous mode, it

increases gradually. After it reaches the maximum velocity value, it remains the same and then gradually decrease to zero when the control mode is switched back to the manual mode.

E. The Supervised Functions

Supervisory functions have been used for autonomous systems, which includes planning, teaching, monitoring, and intervening [20]. The advantages of supervised autonomous control have been demonstrated in [21]. Therefore, we try to incorporate supervised functions in an intervening manner for the autonomous control phase, which leads to the supervised semi-autonomous control.

The supervised functions can be included to the autonomous control as a form of human guidance. Therefore, the operator can maintain control over the robot. The control input from the operator during the autonomous phase can ensure safety during the task execution. Moreover, this enables the dynamic augmentation of the task, which could rectify the uncertainty caused by the unprecise model regression.

The control input is generated by the master controller end-effector position, which is controlled by the operator. While the control output is the additional velocity vector, which can alter the trajectory of the surgical robot end-effector movements during the autonomous task execution phase.

During the autonomous mode, the end-effector of the master robot will remain in the same place, the position of which is $\boldsymbol{p_l}$. Suppose that at time step t, the updated end-effector position controlled by the user is $\boldsymbol{p_m(t)}$. The position control vector $\boldsymbol{p_h(t)}$ generated by the operator is proportional to the master position increment controlled via the master manipulator. $\boldsymbol{p_h(t)}$ is generated by (4).

$$\boldsymbol{p_h(t)} = \boldsymbol{K}(\boldsymbol{p_m(t)} - \boldsymbol{p_l}) \tag{4}$$

where $\boldsymbol{K}$ is a user-specific control mapping factor.

In this way, the supervisory functions can be realized by mapping the displacement and direction from the fixed master device end-effector position to the magnitude and direction of velocity to control the slave robot.

To provide feedback to the operator, the control interface is augmented through force feedback on the regressed path during the autonomous control phase. The feedback $\boldsymbol{F_h(t)}$ can enable the operator to have a sense of how velocity is commanded.

$$\boldsymbol{F_h(t)} = \boldsymbol{Q}(\boldsymbol{p_m(t)} - \boldsymbol{p_l}) \tag{5}$$

where $\boldsymbol{Q}$ is a parameter to enable the user to adjust the force feedback intensity.

In this way, the final control commands are generated by combining both of the desired trajectory and the operator's control input. The final end-effector position can be defined by (6).

$$\boldsymbol{p_s(t)} = \boldsymbol{p_s(0)} + \boldsymbol{p_h(t)} + \boldsymbol{v_a(t)}\Delta t \tag{6}$$

F. Parameters Tuning

Several key parameters for the supervised semi-autonomous control are required to be tuned by the users to reach the optimal control property using the simulator during the surgical training.

1) Robot Control Parameter: This parameter indicates the maximum velocity $\boldsymbol{v}_{max}$ controlled by the robot during the autonomous phase. The autonomous control component is $\boldsymbol{v_a(t)} = \boldsymbol{v}_{max}s(x)$, where $s(x) = \frac{1}{1+e^{-x}}$ is a sigmoid function to make the transition process to be smooth. $s(x)\rightarrow 0$ indicates the entrance of the fully manual control phase.

2) Human Control Parameter: The key parameter of the human-input control component is $\boldsymbol{K}$, which alter the intensity of the supervised function during the autonomous control. $\boldsymbol{K}\rightarrow 0$ indicates fully automatic control, where the supervised function is disabled.

3) Force Rendering Parameter: The force rendering parameter $\boldsymbol{Q}$ can also be tuned, which is the relationship between the haptic feedback and the position increment control commands generated by the operator.

G. Preference-Based Bayesian Optimization

Bayesian optimization is used to find the optimal user-specific parameters. Suppose that m is the number of parameters for optimization, $\boldsymbol{X} \in \mathbb{D}^m$ is the set of user-specific parameters for optimization, $F(\boldsymbol{X})$ is the objective function which is used to evaluate how much benefits of a system can bring to a user. The target is to find out $\boldsymbol{X}_{max}$ = $\underset{\boldsymbol{X}\in\mathbb{D}}{\operatorname{argmax}} F(\boldsymbol{X})$. $F(\boldsymbol{X})$ is a black-box function that does not have a specific meaning, which is only used to represent how the user like the system for preference consideration.

An acquisition function is required to decide where to sample the next data for testing [22]. $E_n[.]$ indicates the expectation taken under the posterior distribution given evaluations of F at $\boldsymbol{X}_m(1\leq m\leq n)$. Suppose that F_{max}=$\max_{m\leq n} F(\boldsymbol{X_m})$. This posterior distribution is given by the GPR.

The next set of parameters for evaluation can be determined by $\boldsymbol{X}_{n+1} = argmax EI_n(\boldsymbol{X})$. The expected improvement (EI) evaluates at the point with the largest expected improvement, which can be calculated as follows.

$$EI = E_n[max(0, F(\boldsymbol{X}) - F_{max})] =$$
$$\begin{cases} Z\sigma(\boldsymbol{X})\Psi(Z) + \sigma(\boldsymbol{X})\Phi(Z), (F_{max} < F(\boldsymbol{X})) \\ 0, otherwise \end{cases} \tag{7}$$

where $Z = \frac{\mu(\boldsymbol{X})-F_{max}}{\sigma(\boldsymbol{X})}$, $\Phi(.)$ represents the probability density function and $\Psi(.)$ represents cumulative distribution function of standard normal distribution ($\mathcal{N} \sim (\mu, \sigma)$).

$\boldsymbol{X = v_{max}, K, Q}$ is used in this paper as variables for fine-tuning. The range of v_{max} is set to be ranged from $3mm/s$ to $9mm/s$, while the K and Q are set to be ranged from 0.6 to 1.8 and -1.5 to -3.5 respectively. For the initial test, we defined the parameters $v_{max} = 6mm/s$, $K = 1.2$, $Q = -2.5$ empirically. The value of the parameters can be adjusted based on the Bayesian optimization protocol, which enables the users to reach the best performance with

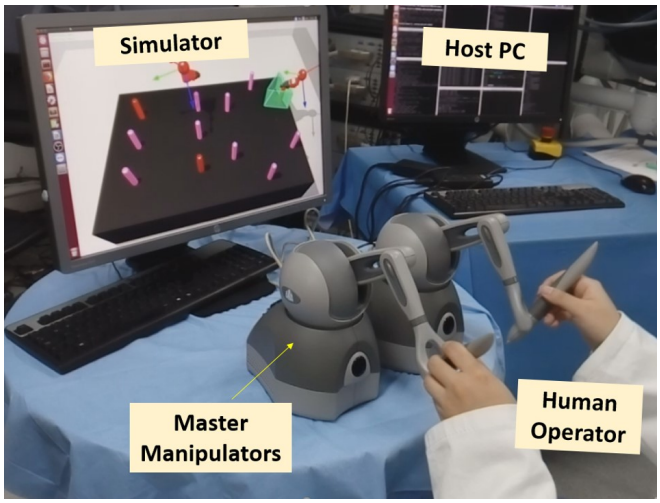

Fig. 3. Overview of the experimental setup and the operational scene.

the desired operation. More technical details of the Bayesian optimization can be found in [10].

III. User Studies

In this section, user studies for validating the proposed framework are introduced, the results of the experiments are analyzed based on several evaluation metrics.

A. Experimental Setup

A customized simulator is developed based on Asynchronous Multi-Body Framework (AMBF) for user studies and user-specific parameters acquisition [23]. For surgical training, compact master manipulators are preferred, instead of using the master manipulators of the original control console [24]. Therefore, two Geomagic Touch devices are used as the compact master manipulators for surgical training.

A peg transfer task was selected for validating the proposed. The peg transfer task is performed using a standard Fundamentals of Laparoscopic Surgery (FLS) training board [25]. In order to reduce the difficulties for participants who do not have surgical operation experience, the task is simplified. The overview of the experimental setup and the operational scene by a subject is shown in Fig. 3.

B. Experimental Protocol

The peg transfer task for the simulator is shown in Fig. 4. The initial position of the right tool is located at A, while the left tool is located parallel to A. The initial position of the grippers are fixed to ensure the comparisons between different trials are fair. The whole procedures for ring transfer task are as follows:

- 1) Control Right gripper to grasp the peg from A, pass it to Left gripper and place it on B.
- 2) Control Left gripper to grasp the peg from B and place it on C.
- 3) Control Right gripper to grasp the peg from C, then place the peg on A.

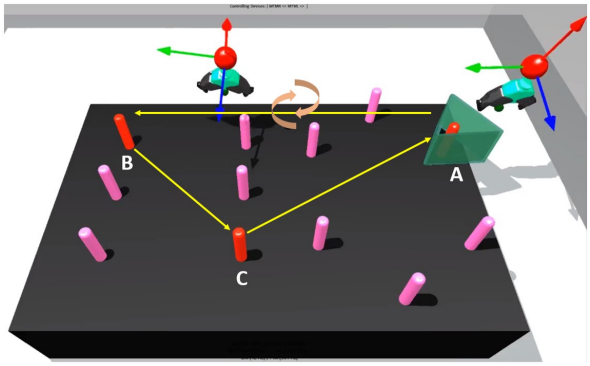

Fig. 4. The simulator for user studies and the illustration of the experimental protocols.

C. User Studies Design

Six subjects were recruited in the user studies. All the participants are right-handed. Two of the subjects have teleoperation experience with the simulator. The first user study was conducted for comparisons between manual control mode and the semi-autonomous control mode. The second user study is developed for comparisons between with and without Bayesian optimization using the supervised semi-autonomous control mode.

Each subject performed the same experiment for three to five trials. Participants are required to use the virtual grippers to grasp, locate, transfer and place the peg in different locations. Experiments would not start until they met the baseline proficiency to be included in the user studies. Then, all the qualified subjects were asked to go through the whole procedure at least twice to get accustomed to the experimental protocols. Once the subjects felt familiar with the control and experimental protocol, task execution began. To obtain a fair comparison, the initial poses of the robot's end-effectors were set to the same value at the beginning.

D. Evaluation Methods

The usability of the proposed method based on user studies is analyzed quantitatively through four evaluation metrics, i.e. i) master robot total trajectory length ($M(m)$), ii) task completion time ($T(s)$), iii) average velocity for the slave robot control ($A(mm/s)$), and iv) number of clutching events (C). To reduce the fatigue of the surgeon during the operation, the smaller $M(m)$ is preferred. Clutching is a process of cutting off the mapping between master and slave and re-centring the master without moving the slave. It is useful when the master manipulator reaches its physical boundary. In pursuit of higher operation efficiency, the less number of clutching and the shorter task completion time and the higher average slave robot control speed can optimize the surgical workflow.

The p-value is used to identify whether the data have significant differences or not. $p < 0.05$ represents that statistic differences can be observed. Normality tests (Shapiro-Wilk test) at 0.05 significance level were performed to verify whether the evaluation metrics have non-parametric

nature or not. Wilcoxon signed-rank tests were conducted for non-parametric statistical comparison between variables (completion time and master robot trajectory), while T-tests were conducted for the other metrics which satisfy the normal distribution assumption. A p-value$<$0.05 is considered significant.

E. Results Analysis

TABLE II
MANUAL CONTROL MODE VS. SEMI-AUTONOMOUS CONTROL MODE

	Manual	Semi-Autonomous	p-value
M (m)	4.72 $\pm$ 1.57	2.37 $\pm$ 1.50	0.0003
T (s)	106.57 $\pm$ 50.84	111.30 $\pm$ 45.00	0.3942
A (mm/s)	9.56 $\pm$ 2.17	10.03 $\pm$ 2.94	0.6215
C	15.9 $\pm$ 6.8	8.0 $\pm$ 6.4	0.0028

TABLE III
WITH VS. WITHOUT BAYESIAN OPTIMIZATION

	Without Optimization	With Optimization	p-value
M (m)	1.48 $\pm$ 0.51	1.44 $\pm$ 0.66	0.2145
T (s)	55.47 $\pm$ 20.64	43.34 $\pm$ 15.03	0.0038
A (mm/s)	11.01 $\pm$ 2.12	12.77 $\pm$ 2.48	0.0280
C	3.3 $\pm$ 2.5	2.4 $\pm$ 1.4	0.0018

Preliminary user studies were conducted for comparisons between manual control mode and semi-autonomous control mode for the simulator. The results are shown in Table II. Results indicated that using the semi-autonomous control mode can reduce the burden of the operator by simplifying the master control trajectory and reducing the clutching frequency significantly. The task completion time and the average slave robot control speed do not have significant differences, which is due to the fact that the maximum velocity control speed is small, while the operator has more freedom to increase the control speed during the fully manual control mode.

The results from user study with Bayesian optimization are obtained by applying different parameters through Bayesian optimization for different subjects. As for the comparisons between with and without using the Bayesian optimization, the results are shown in Table III. Results indicated that with Bayesian optimization, the task completion time is reduced significantly, while the average control speed is enhanced. The total path length of the master trajectory is slightly smaller, but the differences can be overlooked since the p-value is larger than 0.05. The surgical tool trajectories of one study are shown in Fig .5, which illustrates the difference between with and without Bayesian optimization.

National Aeronautical Space Agency-Task Load Index (NASA-TLX) questionnaire is used to measure the subjects' cognitive workload for comparisons between with and without the use Bayesian optimization by scoring six subjective subscales [26], including mental demand, physical demand, temporal demand, performance, effort and frustration. Based on the results of the NASA-TLX, the subjects' cognitive workload could be significantly reduced when using the control method with Bayesian optimization, since the average values of NASA-TLX for the manual optimized mode and the Bayesian tuning mode are 59.32 and 36.86 respectively.

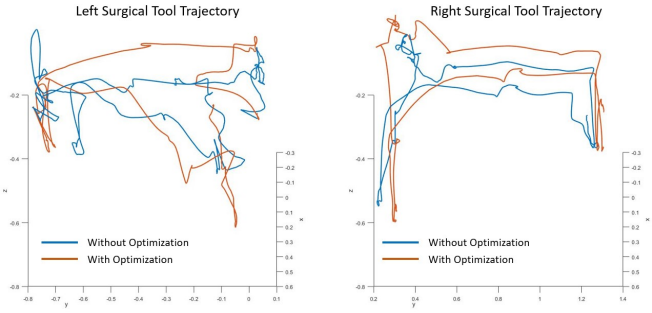

Fig. 5. The trajectory visualization with comparisons between with and without Bayesian optimization.

IV. CONCLUSIONS

This paper presented a supervised semi-autonomous control method for surgical robot control. GPR is used to generate the trajectory for the implementation of autonomous control phase. While the bimanual operation and the interaction with targeted operation areas remain operating in the manual control mode. To verify the effectiveness of the semi-autonomous control method, comparisons were made between manual control mode and semi-autonomous mode using a customized simulator. To identify the efficacy of the Bayesian optimization method, user studies were designed to compare the performance of the operations using the parameters based on with and without Bayesian optimization.

The experiment results indicated that with the supervised semi-autonomous control method, the surgical operation efficiency can be improved. The supervised semi-autonomous control method can exploit the complementary advantages of both the robot and the human operator. The optimal user-specific parameters can be obtained during surgical skill training with the simulator through Bayesian optimization, which can improve the users' performance significantly. The proposed method can reduce the operator's workload, and bring more outcomes.

The supervised semi-autonomous control method can be implemented on other types of surgical platforms with different surgical tools and tasks. Future work will include applying this technique to more complex surgical operations and improve the level of automation.

ACKNOWLEDGEMENT

The authors would like to acknowledge all the subjects for taking part in the user studies. The simulation framework was supported by NSF grants 1637759 and 1927275.

REFERENCES

[1] D. Zhang, J. Liu, L. Zhang, and G.-Z. Yang, "Design and verification of a portable master manipulator based on an effective workspace analysis framework," in *2019 IEEE/RSJ International Conference on Intelligent Robots and Systems (IROS)*. IEEE, 2019, pp. 417–424.

[2] D. Zhang, J. Liu, L. Zhang, and G. Z. Yang, "Hamlyn crm: a compact master manipulator for surgical robot remote control," *International Journal of Computer Assisted Radiology and Surgery*, vol. 15, no. 3, pp. 503–514, 2020.

[3] C. Bergeles and G.-Z. Yang, "From passive tool holders to microsurgeons: safer, smaller, smarter surgical robots," *IEEE Transactions on Biomedical Engineering*, vol. 61, no. 5, pp. 1565–1576, 2014.

[4] D. Zhang, Z. Wu, J. Chen, A. Gao, X. Chen, P. Li, Z. Wang, G. Yang, B. P. L. Lo, and G.-Z. Yang, "Automatic microsurgical skill assessment based on cross-domain transfer learning," *IEEE Robotics and Automation Letters*, 2020.

[5] M. Yip and N. Das, "Robot autonomy for surgery," *arXiv preprint arXiv:1707.03080*, p. 1, 2017.

[6] N. Jarrasse, V. Sanguineti, and E. Burdet, "Slaves no longer: review on role assignment for human–robot joint motor action," *Adaptive Behavior*, vol. 22, no. 1, pp. 70–82, 2014.

[7] M. Power, H. Rafii-Tari, C. Bergeles, V. Vitiello, and G.-Z. Yang, "A cooperative control framework for haptic guidance of bimanual surgical tasks based on learning from demonstration," in *2015 IEEE International Conference on Robotics and Automation (ICRA)*. IEEE, 2015, pp. 5330–5337.

[8] A. D. Pearle, D. Kendoff, V. Stueber, V. Musahl, and J. A. Repicci, "Perioperative management of unicompartmental knee arthroplasty using the mako robotic arm system (makoplasty)," *American Journal of Orthopedics*, vol. 38, no. 2, pp. 16–19, 2009.

[9] J. D. Pitcher, J. T. Wilson, T.-C. Tsao, S. D. Schwartz, and J.-P. Hubschman, "Robotic eye surgery: past, present, and future," *Journal of Computer Science & Systems Biology*, vol. 5, no. 2, p. 1, 2012.

[10] Y. Ding, M. Kim, S. Kuindersma, and C. J. Walsh, "Human-in-the-loop optimization of hip assistance with a soft exosuit during walking," *Science Robotics*, vol. 3, no. 15, p. eaar5438, 2018.

[11] J. Vogel and N. de Freitas, "Target-directed attention: Sequential decision-making for gaze planning," in *2008 IEEE International Conference on Robotics and Automation*. IEEE, 2008, pp. 2372–2379.

[12] T. Matsubara, Y. Funaki, M. Ding, T. Ogasawara, and K. Sugimoto, "Data-efficient human training of a care motion controller for human transfer assistant robots using bayesian optimization," in *2016 6th IEEE International Conference on Biomedical Robotics and Biomechatronics (BioRob)*. IEEE, 2016, pp. 606–611.

[13] W. Chu and Z. Ghahramani, "Preference learning with gaussian processes," in *Proceedings of the 22nd international conference on Machine learning*. ACM, 2005, pp. 137–144.

[14] B. D. Argall, S. Chernova, M. Veloso, and B. Browning, "A survey of robot learning from demonstration," *Robotics and autonomous systems*, vol. 57, no. 5, pp. 469–483, 2009.

[15] H. C. Lin, I. Shafran, D. Yuh, and G. D. Hager, "Towards automatic skill evaluation: Detection and segmentation of robot-assisted surgical motions," *Computer Aided Surgery*, vol. 11, no. 5, pp. 220–230, 2006.

[16] D. Zhang, B. Xiao, B. Huang, L. Zhang, J. Liu, and G.-Z. Yang, "A self-adaptive motion scaling framework for surgical robot remote control," *IEEE Robotics and Automation Letters*, vol. 4, no. 2, pp. 359–366, 2018.

[17] Y. Gao, S. S. Vedula, C. E. Reiley, N. Ahmidi, B. Varadarajan, H. C. Lin, L. Tao, L. Zappella, B. Béjar, D. D. Yuh *et al.*, "Jhu-isi gesture and skill assessment working set (jigsaws): A surgical activity dataset for human motion modeling," in *MICCAI Workshop: M2CAI*, vol. 3, 2014, p. 3.

[18] D. Zhang, J. Chen, W. Li, D. B. Salinas, and G.-Z. Yang, "A microsurgical robot research platform for robot-assisted microsurgery research and training," *International journal of computer assisted radiology and surgery*, vol. 15, no. 1, pp. 15–25, 2020.

[19] M. Seeger, "Gaussian processes for machine learning," *International journal of neural systems*, vol. 14, no. 02, pp. 69–106, 2004.

[20] T. B. Sheridan, *Telerobotics, automation, and human supervisory control*. MIT press, 1992.

[21] A. Shademan, R. S. Decker, J. D. Opfermann, S. Leonard, A. Krieger, and P. C. Kim, "Supervised autonomous robotic soft tissue surgery," *Science translational medicine*, vol. 8, no. 337, pp. 337ra64–337ra64, 2016.

[22] E. Brochu, V. M. Cora, and N. De Freitas, "A tutorial on bayesian optimization of expensive cost functions, with application to active user modeling and hierarchical reinforcement learning," *arXiv preprint arXiv:1012.2599*, 2010.

[23] A. Munawar, Y. Wang, R. Gondokaryono, and G. S. Fischer, "A real-time dynamic simulator and an associated front-end representation format for simulating complex robots and environments," in *2019 IEEE/RSJ International Conference on Intelligent Robots and Systems (IROS)*, Nov 2019, pp. 1875–1882.

[24] D. Zhang, J. Liu, A. Gao, and G.-Z. Yang, "An ergonomic shared workspace analysis framework for the optimal placement of a compact master control console," *IEEE Robotics and Automation Letters*, vol. 5, no. 2, pp. 2995–3002, 2020.

[25] G. Sroka, L. S. Feldman, M. C. Vassiliou, P. A. Kaneva, R. Fayez, and G. M. Fried, "Fundamentals of laparoscopic surgery simulator training to proficiency improves laparoscopic performance in the operating room—a randomized controlled trial," *The American journal of surgery*, vol. 199, no. 1, pp. 115–120, 2010.

[26] S. G. Hart and L. E. Staveland, "Development of NASA-TLX (Task load Index): Results of empirical and theoretical research," in *Advances in psychology*. Elsevier, 1988, vol. 52, pp. 139–183.